An Unusual Open-Framework Cobalt(II) Phosphate with a Channel Structure That Exhibits Structural and Magnetic Transitions**

Amitava Choudhury, S. Neeraj, Srinivasan Natarajan, and C. N. R. Rao*

Among the wide variety of open-framework materials, metal phosphates constitute an important family,[1–4] and interest in these materials is mainly because of potential uses associated with their micoporosity. Open-framework transition metal phosphates are of additional interest because of possible magnetism.[5–12] Magnetic channel structures could have many useful applications, including the separation of oxygen and nitrogen from air. The most common transition metal phosphates are those of iron[5–8], and only a few derivatives of cobalt[9–11] and nickel[12] are known. However, very few open-framework structures with magnetic channels are known to date. Ferri- and ferromagnetic behavior was observed in certain iron phosphates[5–7] and Ni^{II} diphosphonates[13] at low temperatures (less than 10 K). Magnetism in the Ni^{II} diphosphonate arises from a change in the dimensionality and the coordination of the Ni^{II} center on dehydration. Ferrimagnetism was reported in a three-dimensional cobalt succinate[14, 15] at about 10 K, and a metamagnetlike behavior in an organically pillared Co^{II} sulfate.[16] In our pursuit of open-framework metal phosphates with magnetic channels we employed novel synthetic routes to obtain an unusual cobalt(II) phosphate possessing a 12-membered channel with novel structural features and magnetic properties. Interestingly, the cobalt phosphate undergoes a structural phase transition around 170 K followed by the emergence of ferrimagnetism around 16 K. We believe that this is the first observation of such a temperature-induced change in the channel structure of an open-framework metal phosphate.

Open-framework cobalt phosphates are difficult to prepare by the conventional hydrothermal procedure.[17, 18] We therefore employed two routes: with an amine phosphate[19] or a metal amine complex as starting material. Thus, the reaction of Co^{II} ions with diethylenetriamine phosphate (detap) at 180 °C gave $[enH_2][Co_{3.5}(PO_4)_3]$ (**I**) along with a mixture of a few other open-framework cobalt phosphates; the triamine deta decomposed to ethylenediamine (en). The reaction of a mixture with the composition $[Co(en)_3Cl_3]\cdot 2H_2O/2H_3PO_4$/piperazine/150 H_2O at 165 °C for 3 d gave **I** in pure form.[20a] The asymmetric unit of **I** (Figure 1a) contains four crystallographically distinct Co and three P atoms. The final atomic coordinates of **I** at 298 K are given in Table 1. The room-temperature structure consists of a network of CoO_4 [Co(2)], CoO_5 [Co(3), Co(4)], and CoO_6 [Co(1)] polyhedra that are interconnected by PO_4 tetrahedra to form a three-dimensional architecture (Figure 1b). The Co–O and P–O distances are in the ranges 1.931 – 2.427 and 1.499 – 1.573 Å, respectively. The polyhedral connectivity between the various cobalt species in **I** (Figure 2) is such that Co(1) is linked to Co(3) and Co(4) while Co(4) is linked to Co(2) through oxygen atoms to form a secondary building unit (SBU) of composition Co_4O_8. The SBUs are interconnected by phosphate tetrahedra to form a one-dimensional 12-membered elliptical channel of width 6.5×14.2 Å (the longest atom – atom distance not including the van der Waals radii), as shown in Figures 1b and 2a.

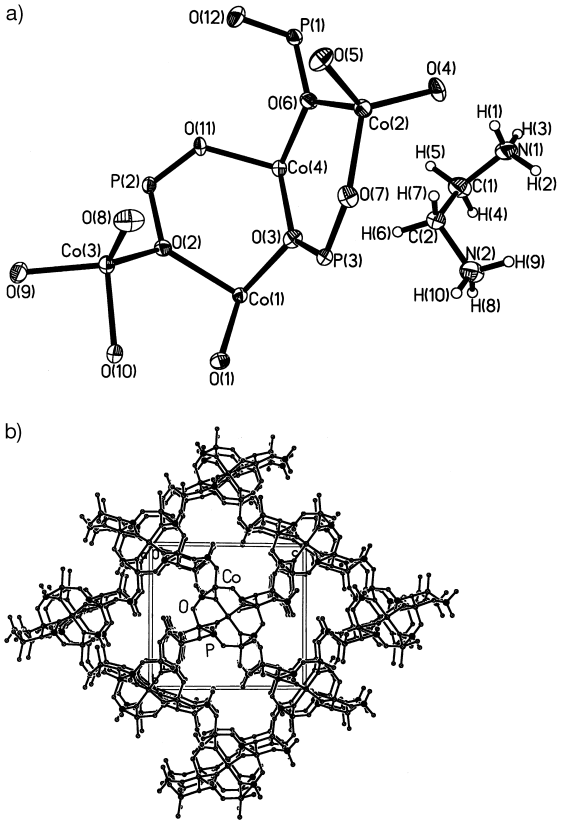

Figure 1. a) Asymmetric unit of **I** at room temperature (50 % probability thermal ellipsoids). b) Structure of **I** along the [100] direction at room temperature showing the 12-membered elliptical channels. The enH_2 cations are omitted for clarity.

A preliminary magnetic susceptibility investigation of **I** in the range 30 – 300 K showed a Curie – Weiss behavior, wherein the slope exhibited a definite change around 200 K. Differential scanning calorimetry (DSC) indicated a phase transition with a small enthalpy change ($\Delta H \approx 20$ cal mol^{-1}) around this temperature. A crystallographic study of **I** at 140 K showed no change in the space group ($P2_1/n$), but changes in the lattice parameters.[20b] The atomic coordinates at 140 K are presented in Table 1. The unit-cell volume at 140 K was significantly larger (ca. 1 %) than at 298 K—a behavior reminiscent of materials with negative coefficients of thermal expansion.[21, 22] The main changes in the structure of **I**

[*] Prof. Dr. C. N. R. Rao, A. Choudhury, S. Neeraj, Dr. S. Natarajan
Chemistry and Physics of Materials Unit and CSIR Centre of Excellence in Chemistry
Jawaharlal Nehru Centre for Advanced Scientific Research
Jakkur P.O., Bangalore 560 064 (India)
Fax: (+91) 80-846-2766
E-mail: cnrrao@jncasr.ac.in
Prof. Dr. C. N. R. Rao, A. Choudhury
Solid State and Structural Chemistry Unit
Indian Institute of Science
Bangalore 560 012 (India)

[**] The authors thank Professor S. K. Malik of the TIFR for help with the SQUID measurements.

  1433-7851/00/3917-3091 $ 17.50+.50/0

Table 1. Atomic coordinates [$\times 10^4$] and equivalent isotropic displacement parameters [Å $\times 10^3$] for **I** at 298 and 140 K.

	298 K				140 K			
Atom	*x*	*y*	*z*	*U*(eq)[a]	*x*	*y*	*z*	*U*(eq)[a]
Co(1)	−10000	0	0	14(1)	−10000	0	0	7(1)
Co(2)	−4655(2)	1771(1)	2836(1)	16(1)	−4654(2)	1771(1)	2835(1)	9(1)
Co(3)	−6543(2)	−1969(1)	815(1)	15(1)	−6567(2)	−1974(1)	822(1)	9(1)
Co(4)	−10085(2)	710(1)	1802(1)	15(1)	−10104(2)	715(1)	1796(1)	8(1)
P(1)	−9154(4)	1008(1)	3699(1)	14(1)	−9151(4)	999(1)	3695(1)	7(1)
P(2)	−10754(4)	−1306(1)	1622(1)	14(1)	−10756(4)	−1305(1)	1622(1)	7(1)
P(3)	−4748(4)	1140(1)	882(1)	18(1)	−4761(4)	1141(1)	875(1)	7(1)
O(1)	−7102(10)	−402(3)	−663(3)	17(1)	−7095(9)	−403(3)	−668(3)	9(1)
O(2)	−9702(10)	−1148(3)	773(3)	17(1)	−9706(10)	−1148(3)	771(3)	9(1)
O(3)	−7543(10)	786(3)	950(3)	23(1)	−7572(10)	794(3)	940(3)	12(1)
O(4)	−6000(11)	2942(3)	2988(3)	22(1)	−6042(10)	2949(3)	2989(3)	13(1)
O(5)	−2164(10)	1105(3)	3572(3)	17(1)	−2178(10)	1095(3)	3572(3)	11(1)
O(6)	−8059(10)	1141(3)	2841(3)	18(1)	−8065(9)	1141(3)	2837(3)	9(1)
O(7)	−3468(10)	1451(3)	1746(3)	27(1)	−3483(10)	1461(3)	1744(3)	11(1)
O(8)	−3630(11)	−1588(4)	1581(3)	22(1)	−3628(10)	−1603(3)	1585(3)	13(1)
O(9)	−7057(11)	−3258(3)	738(3)	17(1)	−7071(10)	−3273(3)	735(3)	11(1)
O(10)	−5229(11)	−1912(3)	−288(3)	17(1)	−5210(10)	−1911(3)	−283(3)	13(1)
O(11)	−10326(11)	−493(3)	2171(3)	20(1)	−10342(10)	−489(3)	2176(3)	13(1)
O(12)	−8330(11)	121(3)	4035(3)	23(1)	−8341(10)	100(3)	4026(3)	13(1)
N(1)	−10214(14)	4305(4)	1880(4)	28(12)	−10167(13)	4286(4)	1896(4)	18(2)
N(2)	−8043(13)	3522(5)	297(4)	28(2)	−8023(12)	3507(4)	286(4)	12(1)
C(1)	−11296(17)	3628(6)	1311(5)	28(2)	−11348(16)	3623(5)	1304(5)	16(2)
C(2)	−9187(17)	3077(5)	984(5)	27(2)	−9211(16)	3065(5)	974(5)	16(2)

[a] *U*(eq) is defined as one third of the trace of the orthogonalized U_{ij} tensor.

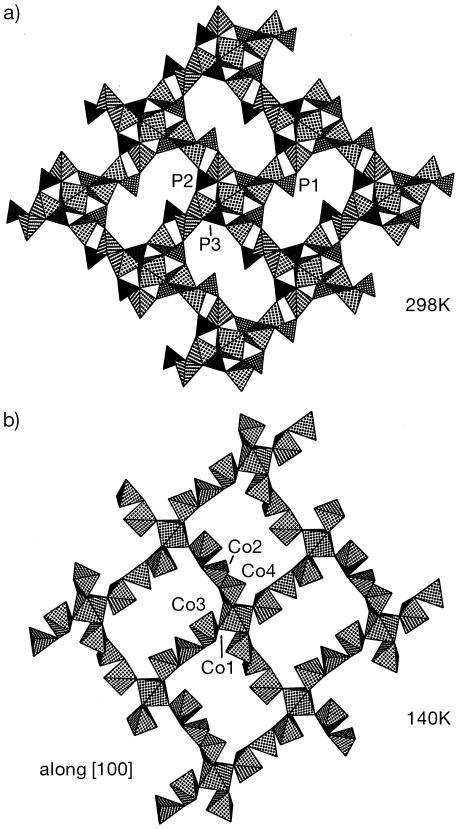

Figure 2. a) The polyhedral connectivity in **I** showing the channels along the *a* axis at 298 K. b) The cobalt – oxygen polyhedral connectivity showing the channels at 140 K.

on cooling occurs around Co(3), especially for the bonds to O(10) and O(4) (Table 2). The Co(3)−O(4) distance is rather long in the room-temperature phase. If we ignore the Co(3)−O(4) bond in the room-temperature phase, the coordination number of Co(3) would change from four to five. If the Co(3)−O(4) bond is taken into account, Co(3) would be essentially unaffected in that it is a pentacoordinate in both the phases, possibly in a trigonal-bipyramidal environment. However, a slight change in the orientation of the enH_2 cations could occur. The Co−Co and Co−P distances in the two phases bear testimony to the structural transition (Table 2). These changes are consistent with the fact that the transition is not truly first order, but is likely to be displacive. Note that the single crystal remains intact across the transition. The face-sharing of the Co(3) and P(2) polyhedra in **I** is rather unusual and is noteworthy. Furthermore, if the Co(3)−O(4) bond is taken into consideration, the structure is three-dimensional. If it is not, the Co network would consist of isolated ribbons shared by PO_4 groups, a situation intermediate between that of magnetic clusters commonly found in porous transition metal phosphates and the Ni phosphates with a three-dimensional Ni network.[12]

Table 2. Some interatomic distances of **I** at 298 and 140 K

	Bond length [Å]	
Moiety	298 K	140 K
Co(3)−O(8)	1.930(5) [0.526][a]	1.940(5) [0.512][a]
Co(3)−O(9)	1.980(5) [0.460]	1.999(5) [0.436]
Co(3)−O(10)	1.987(5) [0.452]	2.007(5) [0.427]
Co(3)−O(2)	2.029(5) [0.402]	2.031(5) [0.400]
Co(3)−O(4)	2.427(5) [0.137]	2.405(5) [0.146]
Co(3)−P(2)	2.809(2)	2.807(2)
Co(2)−P(2)	3.056(2)	3.065(2)
Co(3)−Co(2)	3.620(2)	3.616(2)
Co(2)−O(4)	1.932(5)	1.955(5)
P(2)−O(4)	1.548(6)	1.556(5)

[a] Sum of the bond valences.

The change in the slope of the Curie – Weiss plot of **I** around the structural transition temperature was mentioned above.

  1433-7851/00/3917-3092 $ 17.50+.50/0 *Angew. Chem. Int. Ed.* **2000**, *39*, No. 17

The paramagnetic Curie temperature was calculated as −79 K from susceptibility data in the range 200–300 K, and as −45 K for the range 40–150 K. These values indicate an increase in the ferromagnetic interaction after the structural transition. We examined the low-temperature magnetic properties of the material with a SQUID magnetometer. Figure 3 shows the zero-field-cooled (ZFC) and field-cooled

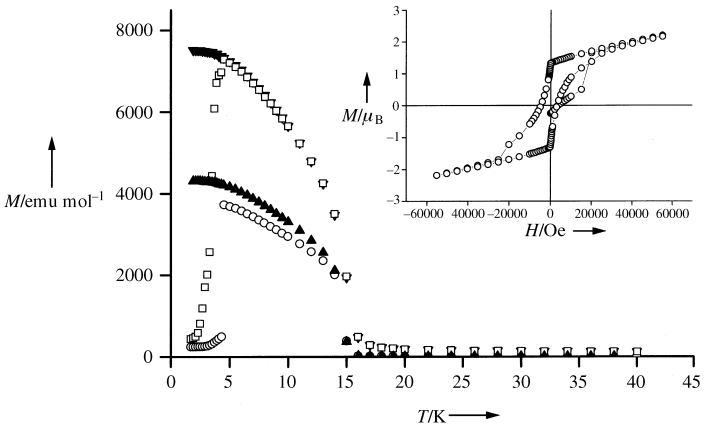

Figure 3. Variation of the magnetic susceptibility of **I** with temperature. The field-cooled (FC) data show a saturation behavior. ○ ZFC, ▲ FC, 50 Oe; □ ZFC, ▼ FC, 1000 Oe. The inset shows the variation of magnetization with the applied field with hysteresis at 2 K. Note the sudden rise in magnetization around 15 kOe.

(FC) magnetization data of the sample at 50 and 1000 Oe. The ZFC data showed a low magnetization at 1.2 K, an abrupt increase between 2 and 4 K on warming, and attainment of a maximum at 4.2 K. It then shows a sharp drop at 16 K where the magnetism vanishes. The drop in magnetization is not found in the FC samples, which exhibit saturation. Such a ferrimagnetic behavior was found recently in a layered Co^{II} hydroxide.[23] The Co-O-Co angles in **I** are in the range of 94–122.4°, which favors ferromagnetic interaction. The angle of 122.4° corresponds to the shared corner of the Co(1) octahedron and the Co(3) trigonal bipyramid. The magnetization versus field plot of **I** shows hysteresis (inset of Figure 3). The magnetization initially rises with increasing field, followed by a sharp jump around 15 kOe. After the jump, the hysteresis loop is that of a typical ferromagnet. Apparently, a transition from one ferrimagnetic to another ferrimagnetic state occurs in a magnetic field; the magnetic moment is too low for a ferromagnetic state.

The isolation of an open-framework Co^{II} phosphate that exhibits a structural phase transition constitutes a novel finding. It is noteworthy that the change in the structure is accompanied by the evolution of ferrimagnetism at low temperatures. We expect that novel routes such as those employed here will enable the synthesis of open-framework structures which are magnetic at considerably higher temperatures.

Received: March 3, 2000 [Z14801]

[1] J. M. Thomas, *Nature* **1994**, *368*, 289.
[2] J. M. Thomas, *Angew.* Chem. **1999**, *111*, 3800; *Angew. Chem. Int. Ed.* **1999**, *38*, 3589.
[3] J. M. Thomas, *Chem. Eur. J.* **1997**, *3*, 1557.
[4] A. K. Cheetham, G. Ferey, T. Loiseau, *Angew. Chem.* **1999**, *111*, 3466; *Angew. Chem. Int. Ed.* **1999**, *38*, 3268.
[5] M. Cavellec, D. Riou, C. Ninclaus, J.-M. Greneche, G. Ferey, *Zeolites* **1996**, *17*, 250.
[6] M. Riou-Cavellec, J.-M. Greneche, G. Ferey, *J. Solid State Chem.* **1999**, *148*, 150.
[7] K.-H. Lii, Y.-F. Huang, V. Zima, C.-Y. Huang, H.-M. Lin, Y.-C. Jiang, F.-L. Liao, S.-L. Wang, *Chem. Mater.* **1998**, *10*, 2599.
[8] A. Choudhury, S. Natarajan, C. N. R. Rao, *Chem. Commun.* **1999**, 1305.
[9] P. Feng, X. Bu, S. H. Tolbert, G. D. Stucky, *J. Am. Chem. Soc.* **1997**, *119*, 2497.
[10] J.-S. Chen, R. H. Jones, S. Natarajan, M. B. Hursthouse, J. M. Thomas, *Angew. Chem.* **1994**, *106*, 667; *Angew. Chem. Int. Ed. Engl.* **1994**, *33*, 639.
[11] J. R. D. DeBord, R. C. Haushalter, J. Zubieta, *J. Solid State Chem.* **1996**, *125*, 270.
[12] N. Guillou, Q. Gao, M. Nogues, R. E. Morris, M. Hervieu, G. Ferey, A. K. Cheetham, *C. R. Acad. Sci. Paris II* **1999**, 387.
[13] Q. Gao, N. Guillou, M. Nogues, A. K. Cheetham, G. Ferey, *Chem. Mater.* **1999**, *11*, 2937.
[14] C. Livage, C. Egger, M. Nogues, G. Ferey, *J. Mater. Chem.* **1998**, *8*, 2743.
[15] C. Livage, C. Egger, G. Ferey, *Chem. Mater.* **1999**, *11*, 1546.
[16] A. Rujiwatra, C. J. Kepert, M. J. Rosseinsky, *Chem. Commun.* **1999**, 2307.
[17] P. Feng, X. Bu, G. D. Stucky, *Nature* **1997**, *388*, 735.
[18] X. Bu, P. Feng, G. D. Stucky, *Science* **1997**, *278*, 2080.
[19] S. Neeraj, S. Natarajan, C. N. R. Rao, *Angew. Chem.* **1999**, *111*, 3688; *Angew. Chem. Int. Ed.* **1999**, *38*, 3480.
[20] a) In a typical synthesis $[Co(en)_3Cl_3]\cdot 2H_2O$ (0.191 g) was dispersed in water (1.35 mL), and H_3PO_4 (85 wt%, 0.07 mL) was added to solution. Then, piperazine (0.043 g) was added with constant stirring to attain a pH of 3.0. The resulting mixture was homogenized for 30 min, transferred into a 23-mL PTFE-lined stainless autoclave, and heated at 165 °C for 72 h. After the reaction, the mixture contained purple-blue needle-shaped crystals of **I**, which were collected by filtration, washed with deionized water, and dried under ambient conditions. A suitable single crystal was subjected to X-ray diffraction studies on a Siemens SMART-CCD diffractometer. Crystal data for **I** (298 K): monoclinic, space group $P2_1/n$ (no. 14), $a=5.0798(1)$, $b=15.2030(4)$, $c=16.3535(1)$ Å, $\beta=95.69(1)^\circ$, $V=1256.7(3)$ Å^3, $Z=4$, $M_r=553.3$, $\rho_{calcd}=2.895$ g cm^{-3}, $\mu(Mo_{K\alpha})=4.955$ mm^{-1}; 5228 reflections were collected at $3.5\le 2\theta\le 46.5^\circ$ and merged to give 1808 unique reflections ($R_{int}=0.08$), of which 1422 with $I>2\sigma(I)$ were considered to be observed. The structure was solved and refined by using the SHELXTL-PLUS suite of programs to $R_1=0.04$, $wR_2=0.1$, and $S=1.13$ for 206 parameters. b) Crystal data for **I** (140 K): monoclinic, space group $P2_1/n$ (no. 14), $a=5.0979(1)$, $b=15.2338(1)$, $c=16.4247(4)$ Å, $\beta=95.67(1)^\circ$, $V=1269.3(3)$ Å^3, $Z=4$, $M_r=553.3$, $\rho_{calcd}=2.895$ g cm^{-3}, $\mu(Mo_{K\alpha})=4.955$ mm^{-1}; 5193 reflections were collected at $3.5\le 2\theta\le 46.5^\circ$ and merged to give 1818 unique reflections ($R_{int}=0.08$), of which 1434 with $I>2\sigma(I)$ were considered to be observed. The structure was solved and refined by using the SHELXTL-PLUS suite of programs to $R_1=0.04$, $wR_2=0.08$, and $S=1.11$ for 206 parameters. Crystallographic data (excluding structure factors) for the structures reported in this paper have been deposited with the Cambridge Crystallographic Data Centre as supplementary publication no. CCDC-141075 (298 K) and -141076 (140 K). Copies of the data can be obtained free of charge on application to CCDC, 12 Union Road, Cambridge CB2 1EZ, UK (fax: (+44) 1223-336-033; e-mail: deposit@ccdc.cam.ac.uk).
[21] T. A. Mary, J. S. O. Evans, T. Vogt, A. W. Sleight, *Science* **1996**, *272*, 90.
[22] M. P. Attfield, A. W. Sleight, *Chem. Commun.* **1998**, 601.
[23] M. Kurmoo, *Chem. Mater.* **1999**, *11*, 3370.

  1433-7851/00/3917-3093 $ 17.50+.50/0